TEC Data Processing Software

Thomas Dautermann, Eric Calais, Purdue University

May 9, 2008

Contents

This documentation describes the GPS data processing software written by Eric Calais and expanded by Thomas Dautermann, Purdue University in the latest revision of March 17th, 2007. The software can be found in */project/hypocenter/j/geodesy/soft/geodesy/iono/tec_17March2007/*

1 GPS Total Electron Content

1.1 Introduction

The Global Positioning System is owned and operated by the United States of America's Department of Defense and Department of Transportation. It is a space-based navigation system intended to provide a user with his exact position anywhere on Earth. According to its organizational structure, the GPS system can be divided into three components: the user segment, the space segment and the control segment. The control segment, currently operated by the US Department of Defense, maintains and controls access to the system. The space segment currently consists of a minimum of 24 satellites in circular orbits of 20,200 km above the earth in 6 orbital planes inclined 55 degrees with respect to the equator and 12 h periods. Each plane is filled with 4 to 6 satellites spaced to guarantee a minimum visibility of 4 satellite at any time at any location on the globe. To eliminate dispersion and refraction effects due to the Earth's ionosphere, the GPS signals are transmitted on two distinct frequencies $f_1 = 1575.42MHz$ and $f_2 = 1227.6MHz$. Each satellite also transmits its own pseudorandom noise code which is used to identify the satellite's signal in the receiver, hence the satellites are usually identified by the prefix PRN followed by the satellite number. The user segment consists of the receiver that uses the signal provided by the satellites to calculate positions. The main observables for scientific purposes are the pseudorange and the carrier phase. The pseudorange is calculated by multiplying the apparent travel time of the GPS signal from a satellite to the receiver with the speed of light. This is not equal to the real satellite-receiver range of the satellite because of a time difference between receiver and satellite clocks and atmospheric delay effects. By means of a phase-lock loop the receiver tracks the number of additional cycles as the satellite moves closer to or further away from the receiver. With the frequencies f_1 and f_2 the wavelength of one cycle is 19 and 24 cm, respectively. Phase tracking provides hence a much higher accuracy for positioning than pseudorange alone. However, the total number of complete cycles between the satellite and receiver is unknown and has to be determined.

1.2 Receiver Composition

As previously mentioned, the basis of the GPS system is the precise measurement of the travel time between satellite and receiver. Each GPS satellite contains a precise cesium clock, whose time stamp is encoded in the GPS navigation signal. In the navigation solution the ground based GPS device receives a minimum of four signals from different satellites. From the travel time of the signal, that is the time difference between receiver clock and satellite clock, a pseudo range ρ is computed by multiplying the travel time with the speed of light. With the four peudoranges, the receiver hardware solves a system of four nonlinear equations and obtains the three position coordinates as well as the time deviation of the receiver clock from the GPS time kept by the satellite chronometers. For a complete description of this technique see for example Misra and Enge (2005) and the references herein. In the solution, corrections for various delays and other effects need to be considered as well. Relativistic corrections due to satellite motion need to be taken into account as well as the effect of the (frequency independent) troposheric delay and the frequency dependent ionospheric delay. For general positioning using a single frequency, a simple model of the ionosphere and atmosphere is employed, giving reasonable accuracy within a few meters. The model corrections among other GPS parameters are described in the GPS Interface Specifications, IS-GPS-200D (2004). In dual frequency positioning, currently a military only application, a linear combination of the two pseudoranges gives a ionosphere-free navigation solution.

An advanced GPS receiver also tracks the carrier phase of the two GPS frequencies by means of a phase lock loop. A phase lock loop contains an internal oscillator wich contiuously adjusts it's frequency and phase to match the one of an incoming signal. As a result the phase lock loop delivers a measurement of the doppler shift of the signal, and the phase difference between the initial lock onto the GPS signal and the current phase of the carrier wave. If the the user can determin the initial number of wavelenths between the GPS satellite and receiver, the carrier phase tracking can be used to obtain a more precise estimate for the position of the receiver.

A typical geodetic GPS receiver records pseudorange ρ_i and carrier phase ϕ_i for both frequencies f_1, f_2 from all satellites in view to an error of 1.5 m (civilian code), 0.2 m (military code) in pseudorange and 0.005 cycles, repectively (Source: Trimble NetRs datasheets *http://www.trimble.com/netrs_ds.asp* and Kaplan (1996), Chapter 7.1.2.6)

1.3 Slant Integrated Electron Content

The ionosphere is a dispersive medium, thus a linear combination of observables on the two frequencies is needed to remove this effect for positioning. On the other hand the dispersive property provides an opportunity to measure directly the ionospheric electron content as first published by Klobuchar (1985) .

The travel time of an electromagnetic wave through a medium with refractive index n is given as

$$t_{travel} = \int_{raypath} \frac{1}{c_{medium}} d\vec{r} = \int_{raypath} \frac{n_{medium}}{c_{vacuum}} d\vec{r} \tag{1}$$

The phase refractive index as a function of the frequency is

$$n^2 = 1 - \frac{\omega_p^2}{\omega^2} \tag{2}$$

where ω_p is the plasma frequency (John D. Jackson, Electrodynamics):

$$\omega_p^2 = \frac{Ne^2}{\epsilon_0 m_e} \tag{3}$$

The refractive index is real and smaller than 1 for $\omega > \omega_p$, thus causing the wave to travel faster than in vacuum. We can expand n in a binomial series that is convergent while $|\frac{\omega_p^2}{2\omega^2}| < 1$. For

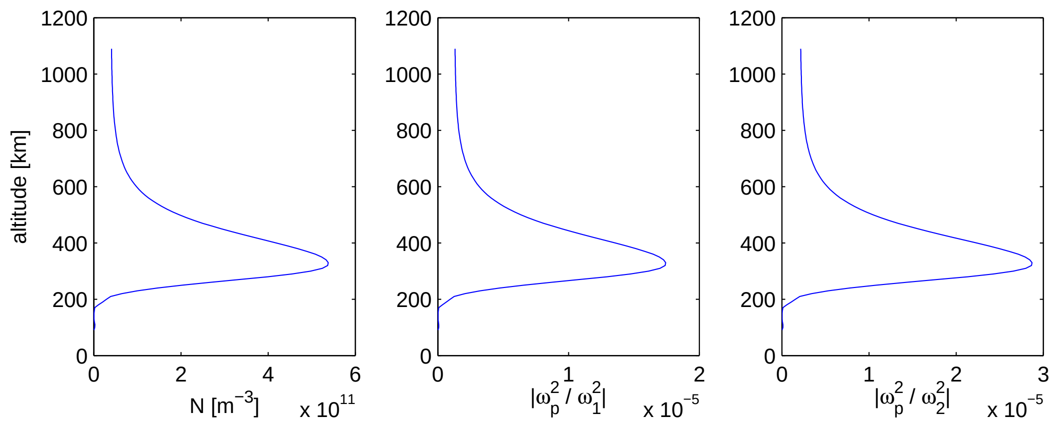

Figure 1: The binomial expansion of (2) is justified, since throughout the ionosphere $|\frac{\omega_p^2}{2\omega^2}| < 1$ (left): typical electron density profile of the ionosphere (center): $|\frac{\omega_p^2}{2\omega^2}|$ for the GPS frequency $\omega_1 = 2\pi f_1$. (right): $|\frac{\omega_p^2}{2\omega^2}|$ for the GPS frequency $\omega_2 = 2\pi f_2$.

a typical value of the electron density in the F-layer of the ionosphere of $N = 5 \times 10^{11} m^{-3}$ and the two GPS frequencies f_1 and f_2 the values of $|\frac{\omega_p^2}{2\omega^2}|$ are 1.62×10^{-5} and 2.67×10^{-5} respectively. Figure 1 shows the validity of the assumption for the whole ionosphere. We expand (2) and retain terms up to first order:

$$n = 1 - \frac{\omega_p^2}{2\omega^2} \tag{4}$$

Substituting ω_p gives:

$$n = 1 - \frac{Ne^2}{2\epsilon_0 m_e \omega^2} = 1 - \frac{Ne^2}{8\pi^2 \epsilon_0 m_e f^2} \tag{5}$$

with $A = \frac{e^2}{8\pi^2 \epsilon_0 m_e} \approx 40.3 \frac{m^3}{s^2}$,so that

$$t_{travel} = \frac{1}{c} \int\limits_{raypath} 1 - \frac{A}{f^2} N(\vec{r}) d\vec{r} \tag{6}$$

The ionospheric phase delay relative to wave propagation in a vacuum is:

$$I_{Phase} = t_{travel}^{medium} - t_{travel}^{vacuum} = -\frac{A}{f^2 c} \int\limits_{raypath} N(\vec{r}) d\vec{r} \tag{7}$$

i.e.the phase is advanced (minus sign). Using the group refractive index with (4) it follows that

$$n_G = 1 + \frac{\omega_p^2}{2\omega^2} \tag{8}$$

The wave group is delayed by

$$I_{Group} = t_{travel}^{medium} - t_{travel}^{vacuum} = \frac{A}{f^2 c} \int\limits_{raypath} N(\vec{r}) d\vec{r} \tag{9}$$

The group delay is thus equal to the phase advance.

$$I_{Group} = -I_{Phase} \tag{10}$$

The phase of the GPS carrier wave is advanced by the same amount of time that the information in a wave group is delayed. The latter integral in (7) and (9) is simply the electron density integrated along the raypath from satellite to receiver, $IEC = \int N(\vec{r})d\vec{r}$ and is called integrated electron content (IEC) or total electron content (TEC). From here on we will use the two words interchangably.

We can measure the relative delay on the two carrier frequencies (i=1,2) using the GPS observables:

$$f(\Phi_i) = f(\rho_i) = I_2 - I_1 = -\frac{A}{c} \frac{f_1^2 - f_2^2}{f_1^2 f_2^2} IEC \tag{11}$$

The pseudoranges ρ_i measured on the two frequencies by multiplying the apparent travel time (derived from the time difference between receiver and satellite clock) between satellite and receiver with the the speed of light. They can be modeled using the satellite receiver distance ρ, the satellite-receiver clock offset τ and tropospheric delay T:

$$\rho_1 = \rho + c\tau - cI_1 + cT \tag{12}$$
$$\rho_2 = \rho + c\tau - cI_2 + cT \tag{13}$$

The negative sign for the ionospheric correction I_i originates in the dispersive plasma, which causes a signal delay but a carrier phase advance. A linear combination gives

$$\rho_2 - \rho_1 = -c(I_2 - I_1) \tag{14}$$

Putting this back into (11), we get :

$$IEC = -\frac{\rho_2 - \rho_1}{A} \frac{f_1^2 f_2^2}{f_1^2 - f_2^2} = \underbrace{-\frac{\rho_2 - \rho_1}{\lambda_2}}_{P_G} \frac{f_1^2 f_2}{(f_1^2 - f_2^2)} \frac{c}{A} \tag{15}$$

We call this linear combination P_G. This provides a measurement for the absolute IEC. Pseudorange measurements are however much noisier and less precise than phase measurements, hence P_G is also much less precise than its equivalent, L_G, derived from the carrier phase measurements. The phase observables can be modeled (in cycles):

$$\Phi_1 = \frac{\rho}{\lambda_1} + f_1\tau + f_1 I_1 + f_1 T + N_1 \tag{16}$$

$$\Phi_2 = \frac{\rho}{\lambda_2} + f_2\tau + f_2 I_2 + f_2 T + N_2 \tag{17}$$

Each phase measurement carries an unknown ambiguity N_i caused by the initial lock onto the signal. Forming a linear combination of the phase observables, it is possible to eliminate most of the unknowns.

$$L_G = \Phi_2 - \frac{f_2}{f_1}\Phi_1 = \underbrace{f_2(I_2 - I_1)}_{=\frac{A}{c}\frac{f_1^2-f_2^2}{f_1^2 f_2}IEC} + N \tag{18}$$

with

$$N = \frac{f_2}{f_1}N_1 - N_2. \tag{19}$$

The ambiguities are constant for a single arc over the receiver site by a single satellite. Moving N to the right hand side yields:

$$\begin{aligned} L_{GU} &= f_2(I_2 - I_1) = L_G - N \\ &= \frac{A}{c}\frac{f_1^2 - f_2^2}{f_1^2 f_2}IEC \end{aligned} \tag{20}$$

We substitute into equation (11) and solve for IEC:

$$IEC = L_{GU}\frac{f_1^2 f_2}{f_1^2 - f_2^2}\frac{c}{A} \tag{21}$$

In the above equation $\frac{f_1^2 f_2}{f_1^2-f_2^2}\frac{c}{A}$ has a value of approximately $2.3 \times 10^{16} m^{-2}$; We used in the following the unit TECU (for total electron content units), where $1\ TECU = 10^{16} m^{-2}$. Since there is no phase ambiguity in P_G because ρ_1 and ρ_2 are absolute pseudoranges, they provide an absolute measurement of the IEC and we can calculate the ambiguity constant N for each satellite pass using the average difference between L_G and P_G over all available epochs for each arc.

$$N = \frac{1}{m}\sum_{i=1}^{m}(P_G - L_G) \tag{22}$$

Using $\Delta\Phi_i = 0.005$ and $\Delta\rho_i = 0.2m$ as previously mentioned in section 1.2 we obtain for the measurement error

$$\Delta P_G = \frac{1}{\lambda_2}\sqrt{\Delta\rho_1^2 + \Delta\rho_2^2} = 0.81m \tag{23}$$

$$\Delta L_G = \sqrt{\Delta\Phi_1^2 + (\frac{f_2}{f_1})^2\Delta\Phi_2^2} = 0.006 \tag{24}$$

For a typical 6 hour GPS satellite pass we have $m \approx 720$ and hence

$$\Delta N = \frac{1}{\sqrt{m}}\sqrt{\Delta P_G^2 + \Delta L_G^2} = 0.043 \tag{25}$$

$$\Delta L_{GU} = \sqrt{\Delta L_G^2 + \Delta N^2} = 0.044 \tag{26}$$

which results in a measurement error of

$$\Delta IEC = \sqrt{\Delta L_{GU}^2 \left[\frac{f_1^2 f_2}{f_1^2 - f_2^2}\frac{c}{A}\right]^2} = 0.102\ TECU \tag{27}$$

if N is estimated. If one is only interested in relative variations, we ignore N and compute only the biases IEC using L_G instead of L_{GU} and the error decreases to

$$\Delta IEC = \sqrt{\Delta L_G^2 \left[\frac{f_1^2 f_2}{f_1^2 - f_2^2}\frac{c}{A}\right]^2} = 0.0147\ TECU \tag{28}$$

1.4 IEC Mapping Technique

The IEC is valid for line of sight from the receiver on the ground to the satellite. Assuming the free electrons concentrated in a thin shell at the height of the main electron concentration in the ionosphere h_I, it can be converted to a vertical electron content (VEC), using an elevation mapping function $E(\Theta)$, which accounts for the different ray path length through the atmosphere as the satellite elevation angle Θ from the receiver and Θ' from the ionospheric height varies . The angle ξ and ξ' denote the zenith angle, which is complementary to the elevation angle, e.g. $\xi = \frac{\pi}{2} - \Theta$.

$$VEC = IEC \cdot E(\Theta) \ = \ IEC \cdot E(\xi) \tag{29}$$

$$E(\xi) \ = \ cos(\xi') \tag{30}$$

From figure 2 the law of sines yields

$$\frac{\sin(\pi - \xi)}{R_E + h_I} \ = \ \frac{\sin \xi'}{R_E} \tag{31}$$

$$\sin \xi' \ = \ \sin \xi \frac{R_E}{R_E + h_I} \tag{32}$$

$$\cos \xi' \ = \ \sqrt{1 - \left(\frac{\sin \xi R_E}{R_E + h_I}\right)^2} \tag{33}$$

$$E(\Theta) \ = \ \sqrt{1 - \left(\frac{\sin(\frac{\pi}{2} - \Theta) R_E}{R_E + h_I}\right)^2} \tag{34}$$

The projection of the point where the line of sight crosses the thin ionospheric shell onto the Earth's surface is called a sub-ionospheric point (SIP). Assuming a spherical Earth it is calculated using the cosine theorem of spherical trigonometry with η and λ denoting latitude and longitude respectively:

$$\gamma = \pi - \xi' - (\pi - \xi) = \xi - \xi' \tag{35}$$

$$\sin(\eta_{sip}) = \sin(\eta_{site}) \cos \gamma + \cos(\eta_{site}) \sin \gamma \cos \alpha \tag{36}$$

$$\cos(\Delta\lambda) = \frac{\cos \lambda \sin(\eta_{sip}) \sin(\eta_{site})}{\cos(\eta_{sip}) \cos(\eta_{site})} \tag{37}$$

where $\Delta\lambda = \lambda_{sip} - \lambda_{site}$ and α denotes the azimuth of the line of sight from north clockwise from 0 up to 2π.

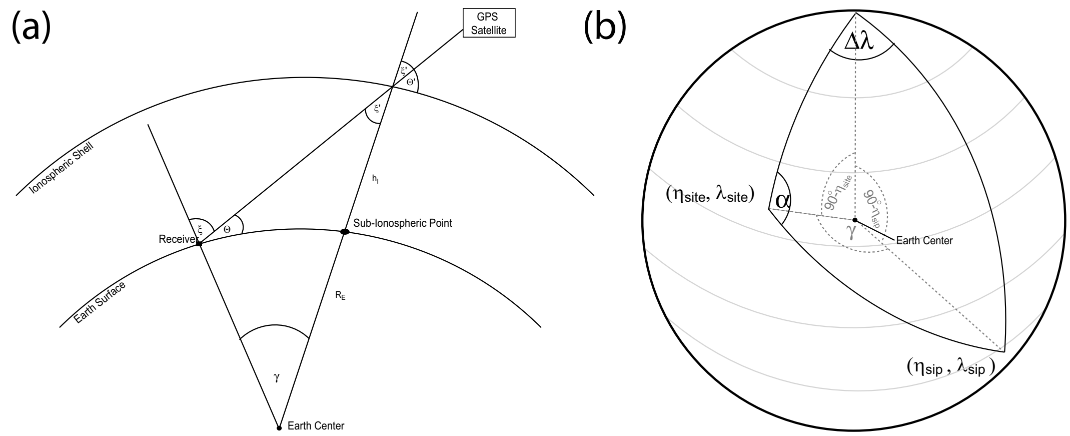

Figure 2: (a) Geometry of the ionospheric mapping, cut through the earth along the a great circle parallel to the line of sight from receiver to satellite. (b) spherical triangle used for SIP calculations

1.5 Correcting Hardware Induced Differential Delay Biases

A non-negligible error source in computing absolute TEC is introduced by the different travel time of the GPS signal on the two separate frequencies through the analogue hardware of satellite and receiver, respectively, which produced a constant TEC bias. The relative delay on the satellite if called transmitter group delay t_{TGD}, the delay caused by the receiver is called receiver inter-frequency bias t_{IFB}

$$t_{IFB} = \delta t_r(f_2) - \delta t_r(f_1) \tag{38}$$

$$t_{TGD} = \delta t_s(f_2) - \delta t_s(f_1) \tag{39}$$

where t_r denotes the travel time through the receiver and t_s the travel time through the satellite hardware, both frequency dependent. Typical values for t_{IFB} are from -20 to 20 ns, with a constant offset of 2.8 $\frac{TECU}{ns}$.

We have to modify equation (20) to

$$\underbrace{I_2 - I_1 - \frac{N}{f_2}}_{=L_{GU}/f_2} + t_{TGD} + t_{IFB}$$

$$= A\frac{f_1^2 - f_2^2}{cf_1^2 f_2^2} IEC \tag{40}$$

We substitute (29) into (40) and call the bias free mapped IEC value the total electron content or TEC.

$$L_{GU}/f_2 + t_{TGD} + t_{IFB} = \frac{A}{E(\Theta)} \frac{f_1^2 - f_2^2}{cf_1^2 f_2^2} TEC \tag{41}$$

Equation (41) is under-determined with the three unknowns IEC (one for each satellite receiver pair and epoch), t_{TGD} (one per satellite), t_{IFB} (one per receiver). At any epoch a single receiver records data from 4 to 12 satellites, the individual satellites are denoted by an index j. The transmitter group delay is broadcast within the navigation message of the GPS satellite and hence known. Using (41) yields the following system of equations:

$$L^j_{GU} - f_2 t^j_{TGD} = \frac{K}{E^j_\Theta} TEC^j - f_2 t_{IFB} \tag{42}$$

using $K = A\frac{f_1^2 - f_2^2}{c f_1^2 f_2}$ With the unknowns TEC and t_{IFB}. The system as is cannot be solved. However, when we map the line of sight measurement to the vertical, each measurement from high elevation satellites should yield the approximate same TEC values assigned to the location above the site of the receiver. We assume a single TEC. Now the system is overdetermined, we write

$$L = Ax \tag{43}$$

The coefficient matrix for this linear system of equations is

$$A = \begin{pmatrix} \frac{K}{E^1_\Theta} & -f_2 \\ \frac{K}{E^2_\Theta} & -f_2 \\ \frac{K}{E^3_\Theta} & -f_2 \\ \vdots & \vdots \end{pmatrix} \tag{44}$$

The data vector $\vec{L}$ contains the the unbiased observables for each satellite $\vec{L}^j_{GU}$ corrected for the transmitter group delay $L^j = L^j_{GU} - f_2 t_{TGD}$ and the vector of unknowns, is defined as:

$$X = \begin{pmatrix} TEC \\ t_{IFB} \end{pmatrix} \tag{45}$$

A straight forward application of this technique is demomstrated in Dautermann et al. (2007), where we searched 2 year absolute TEC time series for statistical connections to earthquakes. The publication is included in this thesis after the Vita.

If the assumption that the electron content does not vary over short distances cannot be made, we can calculate a vertical IEC (VEC) without the correction for the inter-frequency bias.

Other than the simple least squares inversion techniques, other approaches to estimating the biases have been taken: Coco at al. (1991). perform an estimation in the early phase of an incomplete GPS constellation with 5 satellites from 1989 to 1990 using a local quadratic model for the TEC and using a least-squares method developed by Lanyi and Roth (1988) to solve for the combined satellite plus receiver bias. Later on, more crude than our localized least squares technique, Graposchkin and Coster (1993) assume the whole ionosphere to be horizontally stratified at each epoch, before performing the inversion. They do calculate separate receiver and satellite biases. Wilson and Mannucci (1993) use two separate approaches to the problem. The first one uses surface harmonics fitted to 24 h of TEC data as model, the second one, described in detail in Mannuci and Wilson (1993), assumes the ionosphere to be constant at any epoch within a cell on a triangular grid of 642 vertices covering the whole globe. Similar to Coco et al., Sardon et al. (1994) perform the calculations for a TEC model linearly dependent on the position in an earth centered,sun fixed coordinate system. Continuing this study, Sardon and Zarraoa (1997) study the behavior of the biases over 19 months determining the bias to be stable within 1 ns for the receivers and 0.5 ns for the satellites used during that time period. They also determine anti-spoofing not to be a factor in the bias determination. Ma and Maruyama (2003) use the Japanese GEONET, a dense GPS network consisting of 1200 permanent GPS sites. The ionosphere is modeled as a thin shell at the height of the F2 layer. Similarly to Mannuci and Wilson (1993), the shell is gridded in 2^o by 2^o squares and the TEC is assumed to be constant within each cell over 15 minute intervals. One receiver is chosen to have zero bias and all other unknowns are estimated using least squares inversion.

2 Required Input Data

2.1 Rinex GPS Data

GPS data usually provided in the Reciever INdependent EXchange (Rinex) format. Rinex data files are named sitedddf.yyo , where site is a 4-character station name identifier, ddd the day of the year of first record, f the file sequence number within day (usually 0, file contains all the existing data of the current day) and yy are the last 2 digits of the year. The typical rinex file consits of a header with information about the site (i.e. receiver type, antenna type, coordinates,...) and the recorded data (satellites observed, recorded data types) and a data section. The data section contains for each epoch the time of the epoch, satellites with observations, and the observables. For a detailed description of the rinex format see *http://gps.wva.net/html.common/rinex.html* Rinex files are sometimes compressed with the Hatanaka algorithm, wich reduces redundant information from the rinex file. Hatanaka compressed rinex files are identified by the suffix 'd' instea of 'o'. Decompression software is obtained from *ftp://terras.gsi.go.jp/software/RNXCMP_2.4.2/*.

2.2 IGS Orbit Data

The orbit files of the International Geodetic Service (IGS) contain the positions of the GPS satellites for a specific day. They are derived from GPS receivers around the world, whose position is accurately known. Depending on the desired precision the files are available with different latency times.

Orbit	Orbit Acc.	Clock Acc.	Latency	Updates	Sample Int.
Broadcast	160 cm	7ns	real time		daily
Ultra-Rapid (predicted half)	10 cm	5ns	real time	four times daily	15 min
Ultra-Rapid (observed half)	<5 cm	0.2ns	3 hours	four times daily	15 min
Rapid	<5 cm	0.1ns	17 hours	daily	15 min
Final	<5 cm	<0.1ns	≈13 days	weekly	15 min

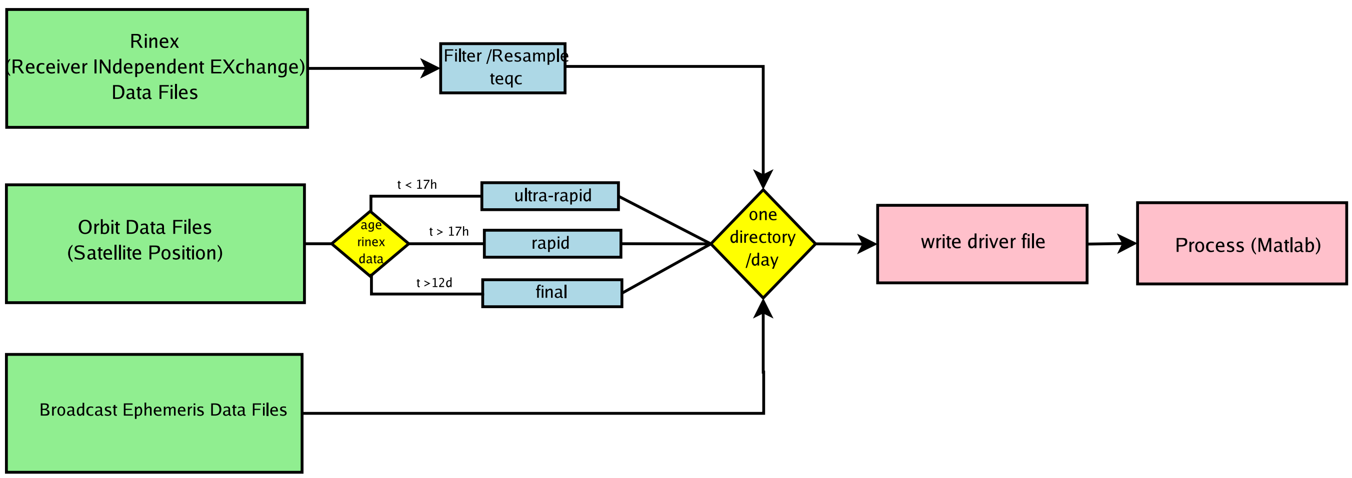

Figure 3: Schematic Diagramm of the process acquiring the required data and prepare for processing

2.3 Data Gathering and Processing Preparation

Figure 3 describes the step to be taken before the GPS data can be processed with the get_tec code. The Rinex data files, once downloaded and decompressed are filtered with the utility program teqc, available at the UNAVCO website, *http://facility.unavco.org/software/teqc/teqc.html*. With the Teqc filtering unwanted data such as signal to noise ratio for the two frequencies is removed as it will confuse the program which reads the data during the processing. Teqc also sets the sampling intervall to the same value for all files being processed together. Depending on the time elapsed since the recording of the data, different qualities of orbit data is available (see Section 2.2). The orbit data with the highest accuracy available should be used. The broadcast ephemerides contain the transmitter group delay for each satellite. This file is only necessary if the total electron content is computed. Once all data is locally present a driver file required by the Matlab processing is written. It contains processing parameters and the input file names.

3 Main Program Components

3.1 Processing Flow

The main processing code is contained in the file get_tec.m. Figure 4 illustrates the steps during the TEC calculations. Get_tec is run with the driver file as input parameter. It then reads and interpolates the orbit data to match the sampling of the GPS observables and retrieves the transmitter group delay from the ephemerides file. The IEC (biased for the receiver inter-frequncy bias) and supplemental data are now calculated for each site. Rinex data is read with the readrinex MEX file, the IEC calculated according to equation 21. Now we calculate the positions of the SIPs for each epoch according to equations (36) and (37).

The data is then sorted an reorganized in a structure 'data_site' with fields for each satellite observed. This structure can optionally be saved as a Matlab data file. If the user choses to compute

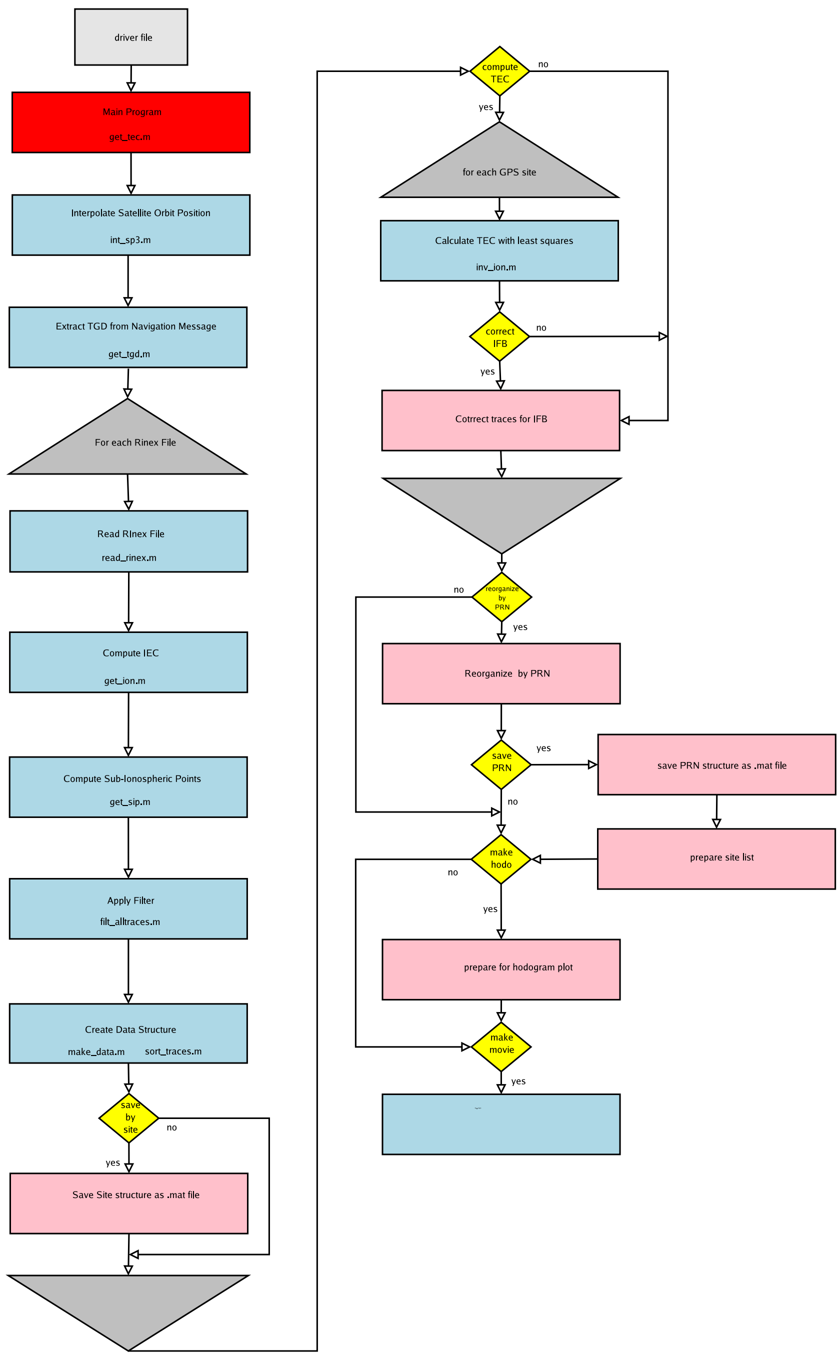

Figure 4: TEC processing code including optional calculations

the absolute TEC for each station, the least squares solution for equation (43) is obtained for each site. With the calculated IFB the IEC calculated before can be corrected. If many stations are processed for a particular day it may be advisable to reoganize the data by satellite instead of by station and then save this structure. The user can choose to generate Hodograms using the Generic Mapping Tools (GMT).

3.2 get_tec.m

This is the main program code. It can be run as a script or as a function with the driver file as an argument get_tec('driverfile'). The driver file is a text file, which contains a list of all the data files, orbit file and broadcast ephemerides file as well as some processing parameters such as sampling interval, altitude of the ionospheric shell for sub ionospheric point calculation, event location and event time.

```
Oregon Bolide       % comment
1330                % time of event (hours UT)
45.786580           % latitude of event
-118.191420         % longitude of event
40 50               % latitude range for SIP map (not used)
-110 -130           % longitude range for SIP map (not used)
12 16               % time window
30                  % sampling interval
02192008            % date
10                  % elevation cutoff
6.0                 % magnitude (not used)
0.0                 % depth (not used)
325000              % alt_ion = ionospheric height (meters)
-58.369             % magnetic inclination at alt_ion (degres) (not used)
13.532              % magnetic declination at alt_ion (degres) (not used)
1000                % maximum distance from source to consider (km) (not used)
50                  % step for distance to source (km) (not used)
y                   % filter data
b                   % filter type
2.2 8               % filter limit (mHz)
n                   % make hodo
y                   % reorganize prn
n                   % compute tec
y                   % save as mat
y                   % save prn as mat
y                   % clean data
n                   % correct IFB
n                   % write TECfile
CODG0500.08I        % ionex file
```

```
epgga8.050          % ephemerides file
igs14672.sp3        % orbit file
p0200500.08o        % data file
p0220500.08o        % data file
p3720500.08o        % data file
p3860500.08o        % data file
p3940500.08o        % data file
p4220500.08o        % data file
p4450500.08o        % data file
p4470500.08o        % data file
p4480500.08o        % data file
p4490500.08o        % data file
p4510500.08o        % data file
p4520500.08o        % data file
```

The non self explanatory options in the driver file are:

- cutoff is the value(s) for the filter cut-off in mHz (milli-Hertz)
- f_type is a character describing the filter type (h/b/l)

The following options can be turned on with 'y' for yes and 'n' for no:

- *%filter data* if turned off, the data is not filtered, the unfiltered TEC replaces the filtered one in the output
- *%make hodo* prepares data for plotting a hodogram with GMT
- *%reorganize prn* reorganizes data in structures by prn additionally to the structures by site
- *%compute tec* calculates absolute TEC with a least squares algorithm
- *%save as mat* saves site data structures in .mat files for each site
- *%save prn as mat* saves PRN data structure in mat files, requires %reorganize prn set to 'y'
- *%clean data* filters oscillations in pseudorange and phase, parameters for the cleaning process can be set in clean_obs.m
- *%correct IFB* corrects after calculating tec (compute_tec=='y') the traces in the site data structures for the inter-frequency bias
- *%write TECfile* writes total TEC into a file tec_site.mat, requires %compute tec set to 'y'

The following files are needed:

- *% orbit file* This is the igs orbits mentioned above.
- *% ephemerides file* Broadcast ephemerides. This can be used for extracting transmitter group delay.
- *% ionex file* Postprocessed ionosphere data from the Center for Orbit Determination in Europe from the University of Bern (CH). It has better estimates for the transmitter group delay.
- *% data file* This is the rinex data. While running the code, you may get better results if the data is run through teqc before to assure uniform sampling and eliminate unneccessary observables like Signal-to-Noise ratio or doppler. The teqc command to use is *"teqc -O.obs L1L2C1P1P2 -O.dec 30 purd0230.08o ¿ purd1230.08o"*.

3.3 int_sp3.m

[SAT,sv] = int_sp3(sp3file, splint)

Interpolates the GPS satellite orbits in the orbit file sp3file with extension sp3 from a fifteen minute sampling to splint (in s sampling). for older version of orbit files

int_sp3_new.m

same as int_sp3.m but for newer version of orbit files. Main difference between the two formats is the satellite description: new format is PGXX, old format is P XX where x stands for the satellite number.

3.4 get_tgd.m

tgd = get_tgd(rinexn)

extracts the Transmitter Group Delay tgd from the Rinex navigation file rinexn

3.5 readrinex.c

[Observables,epochs,sv,apcoords]=readrinex(rnx_file);

Mex C-code which reads the data from the rinex data file rnx_file and returns the structure Observables which contains the the data for phase data (L1, L2) on both frequencies and the pseudorange (P1, P2) on both frequencies. Some receivers do not record the precise pseudorange on frequency 1 but rather the coarse civilian signal C1. Each field of the structure observables contains #epochs rows and #satellites columns, no observation is designated by NaN (Not a Number). The time of observation is given int epochs and the satellites with observations are given in sv. The order of sv corresponds to the columns of each field in Observables. apcoords are the site coordinates in earth centered, earth fixed XYZ coordinates from the header of the rinex file.

3.6 get_ion.m

[iec,iec_dot,lgu] = get_ion(L1,L2,C1,P1,P2,sv,tgd)

This computes the the integrated electron content already corrected for the transmitter group delay tgd. SV are the satellites with observations each elements contains a satellite number, which corresponds to a column in the matrix of observables and an the corresponding transmitter group delay in tgd. It returns the values for the integrated electron content seen by each satellite the change in integrated electron content and the unbiased phase observable lgu.

3.7 get_sip.m

SIP = get_sip(SAT,sv,alt_ion,apcoords,Tmin,Tmax,lat_epi,lon_epi,dec,inc)

This subroutine calculates the location of the projection of the ionospheric piecing point onto the WGS84 ellipsoid (called a sub-ionospheric poin or SIP) along with some associated information. It returns a structure SIP with each field describing one satellite containing the time in UT hour of current day, latitude of SIPs in degrees, longitude of SIPs in degrees, elevation with respect tot the GPS site in degrees, azimuth with respect to the GPS site in degrees, distance from event to SIP (m), azimuth from event to SIP (in degrees clockwise from north) and the angle between magnetic direction and satelllite-receiver line-of-sight . The input SAT is the structure containing satellite positions created by int_sp3, sv a vector of PRN numbers created by readrinex. alt_ion describes the height of the ionspheric piercing point. apcoords are coordinates of GPS site (XYZ, m) created by readrinex Tmin and Tmax give a time windows (in hours UT) during which the SIPs are calculated lat_epi, lon_epi are the location of event, dec, inc the declination and inclination of magnetic field in degrees respectively.

3.8 filt_alltraces.m

iec_filt = filt_alltraces(iec,t,splint,cutoff,f_type);

This filters a segment of iec data sampled at splint using a fourth order Butterworth filter with a given cutoff. f_type selects between high-pass, low-pass and band-pass

3.9 sort_traces.m

[SR,SF,SL,sv_new] = sort_traces(iec,iec_filt,lgu,t,sv,exc_sv);

This sorts iec, iec_filt, and lgu arrays and return structures with each field referring to a satellite. SF contains filtered, SR unfiltered IEC, SL is the LGU observable. It also returns sv_new, a new vector with prn numbers

3.10 make_data.m

data = make_data(sr,sf,sl,sip,sv);

make_data merges sr, sf,sl and sip structures from sort_traces into a single structure 'data'. sv is a vector with the list of prn's to consider. The structure data contains a field for each prn with a n x 13 marix the columns containg ins this order time, filtered IEC, raw IEC, time_sip, latitude of the SIP, longitude of the SIP, elevation of the satellite, azimuth of the satellite, distance of SIP from the epicenter, azimuth to the epicenter, angle between magnetic direction and satellite-receiver line-of-sight, elevation mapping function, Lgu Observable

3.11 inv_ion.m

[time_tec,tec,tec_inv,tec_smooth,br] = inv_ion(data,tgd,ele_cut)

Calculates absolute TEC with least squares. data is the data structure from make_data tgd the vector of transmitter group delays from get_tgd, ele_cut denotes the elevation cut-off angle in degrees. The outputs are a integrated electron content from averaging (tec), integrated electron content from inversion (tec_inv, in TECU), a smoothed tec_inv , and the receiver interfrequency bias for the site considered.

4 Plotting and Analysis Utilities

4.1 plot_data.m

plot_data(data,factor,T_eq,threshold,plot_txt,decal)

Plots iec time series from structure data created by makedata.m in time-iec domain scaled by an arbitrary factor sorted by distance of source and SIP at the time of the event (T_eq). It is optional to plot PRN number or SITE name by each trace. decal = 0 will use source-station distance for y-axis n will shift each trace by n km along y-axis.

4.2 plot_sip.m

plot_sip(site_list,lati_site,long_site,lat_epi, lon_epi,lonlim,latlim,T_eq,time_after)

Plots a map of the SIPs for the sites contained in site_list for specified amount of time after the event.

4.3 plot_scatter.m

plot_scatter(data,threshold)

Plots iec time series in actual time-distance domain, the color of the trace indicates the IEC value. The Distance is between source and sip and varies with satellite motion. Per default this plots the filtered iec. A threshold is used to elimnate abnormally high values.

4.4 plot_specgram

plot_specgram(data,field,samp);

Plots a spectrogram of filtered IEC in a field of the stucture data from makedata.m. The spectrogram is created using a 60 point Hanning window with 59 point overlap and ranges from 0.01 mHz to 2.5mHz.

4.5 slant_stack.m

[T,STACK,max_amp,n_traces] = slant_stack(data,mov,time_frame,dist_frame,T_eq,splint,N_root)

Slant stacks filtered iec traces given in the structure 'data' sampled at splint s, using moveout velocity 'mov' (m/s). The stack is done in a window defined by 'time_frame' (dec. hours) and 'dist_frame' (m). Nth root process slant stack is possible with N_root =1. Use N_root = 1 for linear slant stack.

4.6 swap_filt.m

data = swap_filt(data,cutoff,f_type,splint);

Calculates time series filtered with new filter and replaces the corresponding entry in the 'data' structure. For details see section 3.8.

4.7 swap_dist.m

data = swap_dist(data,lat_epi,lon_epi);

Calculates new distance for each SIP from the new coordinates specified with lat_epi and lon_epi and swaps the corresponding entry in the 'data' structure (see section 3.7).

4.8 plot_raw.m

plot_raw(iecStruct,offset)

Plots the raw TEC for a given structure. It can be shifted by a constant tec offset. Use to visualize diurnal variations for a given site.

References

[1] C. Coco, D.S.and Coker, S.R. Dahlke, and J.R. Clynch. Variability of GPS satellite differential group delay biases. *IEEE Transactions on Aerospace and Electronic Systems*, 27(6):931–938, November 1991.

[2] E. M Gaposchkin and A.J. Coster. GPS L1-L2 bias determination. Technical Report 971, MIT Lincoln Laboratory, 1993.

[3] IS-GPS-200D. Navstar GPS Space Segment/Navigation User Interfaces, Revision D. Technical Report IS-GPS-200D, GPS Joint Program Office, December 2004.

[4] J.D. Jackson. *Classical Electrodynamics*. Wiley, New York, 1998.

[5] Elliot D. Kaplan. *Understanding GPS - Principles and Applications*. Artech House Publishers, Norwood, MA, 1996.

[6] J. A. Klobuchar. Ionospheric time delay effects on earth space propagation. In A. S. Jursa, editor, *Handbook of Geophysics and the space evironment*, chapter 10.8, pages 1084–1088. U.S. Air Force, Washingto, D.C., 1985.

[7] G. E. Lanyi and T. Roth. A comparison of mapped and measured total ionospheric electron content using global positioning system and beacon satellite observations. *Radio Science*, 23:483–492, August 1988.

[8] G. Ma and T. Maruyama. Derivation of TEC and estimation of instrumental biases from GEONET in Japan. *Annales Geophysicae*, 21(10):2083–2093, October 2003.

[9] Anthony J. Manucci, Brian D. Wilson, and Charles D. Edwards. A new method for monitoring the Earth's ionospheric total electron content using the GPS global network. In *ION GPS-93: Proceedings of the 6th International Technical Meeting of the Satellite Division of the Institute of Navigation*, pages 1323–1332, Salt Lake City, UT, USA, September 1993.

[10] Pratap Misra and Per Enge. *Global Positioning System: Signals, Measurements and Performance*. Ganga-Jamuna Press, Lincoln, Massachusetts, 2004.

[11] E. Sardón and N. Zarraoa. Estimation of total electron content using GPS data: How stable are the differential satellite and receiver instrumental biases? *Radio Science*, 32(5):1899–1910, 1997.

[12] Brian D. Wilson and Anthony J. Mannucci. Instrumental Biases in Ionospheric Measurements Derived from GPS Data. In *ION GPS-93: Proceedings of the 6th International Technical Meeting of the Satellite Division of the Institute of Navigation*, pages 1343–1351, Salt Lake City, UT, USA, September 1993.